

Measurement of the Lepton Charge Asymmetry in W -Boson Decays Produced in $p\bar{p}$ Collisions

F. Abe,¹⁷ H. Akimoto,³⁹ A. Akopian,³¹ M. G. Albrow,⁷ A. Amadon,⁵ S. R. Amendolia,²⁷ D. Amidei,²⁰ J. Antos,³³ S. Aota,³⁷ G. Apollinari,³¹ T. Arisawa,³⁹ T. Asakawa,³⁷ W. Ashmanskas,¹⁸ M. Atac,⁷ P. Azzi-Bacchetta,²⁵ N. Bacchetta,²⁵ S. Bagdasarov,³¹ M. W. Bailey,²² P. de Barbaro,³⁰ A. Barbaro-Galtieri,¹⁸ V. E. Barnes,²⁹ B. A. Barnett,¹⁵ M. Barone,⁹ G. Bauer,¹⁹ T. Baumann,¹¹ F. Bedeschi,²⁷ S. Behrends,³ S. Belforte,²⁷ G. Bellettini,²⁷ J. Bellinger,⁴⁰ D. Benjamin,³⁵ J. Bensinger,³ A. Beretvas,⁷ J. P. Berge,⁷ J. Berryhill,⁵ S. Bertolucci,⁹ S. Bettelli,²⁷ B. Bevensee,²⁶ A. Bhatti,³¹ K. Biery,⁷ C. Bigongiari,²⁷ M. Binkley,⁷ D. Bisello,²⁵ R. E. Blair,¹ C. Blocker,³ S. Blusk,³⁰ A. Bodek,³⁰ W. Bokhari,²⁶ G. Bolla,²⁹ Y. Bonushkin,⁴ D. Bortoletto,²⁹ J. Boudreau,²⁸ L. Breccia,² C. Bromberg,²¹ N. Bruner,²² R. Brunetti,² E. Buckley-Geer,⁷ H. S. Budd,³⁰ K. Burkett,²⁰ G. Busetto,²⁵ A. Byon-Wagner,⁷ K. L. Byrum,¹ M. Campbell,²⁰ A. Caner,²⁷ W. Carithers,¹⁸ D. Carlsmith,⁴⁰ J. Cassada,³⁰ A. Castro,²⁵ D. Cauz,³⁶ A. Cerri,²⁷ P. S. Chang,³³ P. T. Chang,³³ H. Y. Chao,³³ J. Chapman,²⁰ M.-T. Cheng,³³ M. Chertok,³⁴ G. Chiarelli,²⁷ C. N. Chiou,³³ F. Chlebana,⁷ L. Christofek,¹³ M. L. Chu,³³ S. Cihangir,⁷ A. G. Clark,¹⁰ M. Cobal,²⁷ E. Cocca,²⁷ M. Contreras,⁵ J. Conway,³² J. Cooper,⁷ M. Cordelli,⁹ D. Costanzo,²⁷ C. Couyoumtzelis,¹⁰ D. Cronin-Hennessy,⁶ R. Culbertson,⁵ D. Dagenhart,³⁸ T. Daniels,¹⁹ F. DeJongh,⁷ S. Dell'Agnello,⁹ M. Dell'Orso,²⁷ R. Demina,⁷ L. Demortier,³¹ M. Deninno,² P. F. Derwent,⁷ T. Devlin,³² J. R. Dittmann,⁶ S. Donati,²⁷ J. Done,³⁴ T. Dorigo,²⁵ N. Eddy,²⁰ K. Einsweiler,¹⁸ J. E. Elias,⁷ R. Ely,¹⁸ E. Engels, Jr.,²⁸ W. Erdmann,⁷ D. Errede,¹³ S. Errede,¹³ Q. Fan,³⁰ R. G. Feild,⁴¹ Z. Feng,¹⁵ C. Ferretti,²⁷ I. Fiori,² B. Flaughner,⁷ G. W. Foster,⁷ M. Franklin,¹¹ J. Freeman,⁷ J. Friedman,¹⁹ H. Frisch,⁵ Y. Fukui,¹⁷ S. Gadomski,¹⁴ S. Galeotti,²⁷ M. Gallinaro,²⁶ O. Ganel,³⁵ M. Garcia-Sciveres,¹⁸ A. F. Garfinkel,²⁹ C. Gay,⁴¹ S. Geer,⁷ D. W. Gerdes,¹⁵ P. Giannetti,²⁷ N. Giokaris,³¹ P. Giromini,⁹ G. Giusti,²⁷ M. Gold,²² A. Gordon,¹¹ A. T. Goshaw,⁶ Y. Gotra,²⁸ K. Goulianos,³¹ H. Grassmann,³⁶ L. Groer,³² C. Grosso-Pilcher,⁵ G. Guillian,²⁰ J. Guimaraes da Costa,¹⁵ R. Guo,³³ C. Haber,¹⁸ E. Hafen,¹⁹ S. R. Hahn,⁷ R. Hamilton,¹¹ T. Handa,¹² R. Handler,⁴⁰ F. Happacher,⁹ K. Hara,³⁷ A. D. Hardman,²⁹ R. M. Harris,⁷ F. Hartmann,¹⁶ J. Hauser,⁴ E. Hayashi,³⁷ J. Heinrich,²⁶ W. Hao,³⁵ B. Hinrichsen,¹⁴ K. D. Hoffman,²⁹ M. Hohmann,⁵ C. Holck,²⁶ R. Hollebeck,²⁶ L. Holloway,¹³ Z. Huang,²⁰ B. T. Huffman,²⁸ R. Hughes,²³ J. Huston,²¹ J. Huth,¹¹ H. Ikeda,³⁷ M. Incagli,²⁷ J. Incandela,⁷ G. Introzzi,²⁷ J. Iwai,³⁹ Y. Iwata,¹² E. James,²⁰ H. Jensen,⁷ U. Joshi,⁷ E. Kajfasz,²⁵ H. Kambara,¹⁰ T. Kamon,³⁴ T. Kaneko,³⁷ K. Karr,³⁸ H. Kasha,⁴¹ Y. Kato,²⁴ T. A. Keaffaber,²⁹ K. Kelley,¹⁹ R. D. Kennedy,⁷ R. Kephart,⁷ D. Kestenbaum,¹¹ D. Khazins,⁶ T. Kikuchi,³⁷ B. J. Kim,²⁷ H. S. Kim,¹⁴ S. H. Kim,³⁷ Y. K. Kim,¹⁸ L. Kirsch,³ S. Klimentenko,⁸ D. Knoblauch,¹⁶ P. Koehn,²³ A. Königeter,¹⁶ K. Kondo,³⁷ J. Konigsberg,⁸ K. Kordas,¹⁴ A. Korytov,⁸ E. Kovacs,¹ W. Kowald,⁶ J. Kroll,²⁶ M. Kruse,³⁰ S. E. Kuhlmann,¹ E. Kuns,³² K. Kurino,¹² T. Kuwabara,³⁷ A. T. Laasanen,²⁹ S. Lami,²⁷ S. Lammel,⁷ J. I. Lamoureux,³ M. Lancaster,¹⁸ M. Lanzoni,²⁷ G. Latino,²⁷ T. LeCompte,¹ S. Leone,²⁷ J. D. Lewis,⁷ P. Limon,⁷ M. Lindgren,⁴ T. M. Liss,¹³ J. B. Liu,³⁰ Y. C. Liu,³³ N. Lockyer,²⁶ O. Long,²⁶ C. Loomis,³² M. Loretì,²⁵ D. Lucchesi,²⁷ P. Lukens,⁷ S. Lusin,⁴⁰ J. Lys,¹⁸ K. Maeshima,⁷ P. Maksimovic,¹⁹ M. Mangano,²⁷ M. Mariotti,²⁵ J. P. Marriner,⁷ A. Martin,⁴¹ J. A. J. Matthews,²² P. Mazzanti,² P. McIntyre,³⁴ P. Melese,³¹ M. Menguzzato,²⁵ A. Menzione,²⁷ E. Meschi,²⁷ S. Metzler,²⁶ C. Miao,²⁰ T. Miao,⁷ G. Michail,¹¹ R. Miller,²¹ H. Minato,³⁷ S. Miscetti,⁹ M. Mishina,¹⁷ S. Miyashita,³⁷ N. Moggi,²⁷ E. Moore,²² Y. Morita,¹⁷ A. Mukherjee,⁷ T. Muller,¹⁶ P. Murat,²⁷ S. Murgia,²¹ H. Nakada,³⁷ I. Nakano,¹² C. Nelson,⁷ D. Neuberger,¹⁶ C. Newman-Holmes,⁷ C.-Y. P. Ngan,¹⁹ L. Nodulman,¹ A. Nomerotski,⁸ S. H. Oh,⁶ T. Ohmoto,¹² T. Ohsugi,¹² R. Oishi,³⁷ M. Okabe,³⁷ T. Okusawa,²⁴ J. Olsen,⁴⁰ C. Pagliarone,²⁷ R. Paoletti,²⁷ V. Papadimitriou,³⁵ S. P. Pappas,⁴¹ N. Parashar,²⁷ A. Parri,⁹ J. Patrick,⁷ G. Pauletta,³⁶ M. Paulini,¹⁸ A. Perazzo,²⁷ L. Pescara,²⁵ M. D. Peters,¹⁸ T. J. Phillips,⁶ G. Piacentino,²⁷ M. Pillai,³⁰ K. T. Pitts,⁷ R. Plunkett,⁷ A. Pompos,²⁹ L. Pondrom,⁴⁰ J. Proudfoot,¹ F. Ptohos,¹¹ G. Punzi,²⁷ K. Ragan,¹⁴ D. Reher,¹⁸ M. Reischl,¹⁶ A. Ribon,²⁵ F. Rimondi,² L. Ristori,²⁷ W. J. Robertson,⁶ T. Rodrigo,²⁷ S. Rolli,³⁸ L. Rosenson,¹⁹ R. Roser,¹³ T. Saab,¹⁴ W. K. Sakumoto,³⁰ D. Saltzberg,⁴ A. Sansoni,⁹ L. Santi,³⁶ H. Sato,³⁷ P. Schlabach,⁷ E. E. Schmidt,⁷ M. P. Schmidt,⁴¹ A. Scott,⁴ A. Scribano,²⁷ S. Segler,⁷ S. Seidel,²² Y. Seiya,³⁷ F. Semeria,² T. Shah,¹⁹ M. D. Shapiro,¹⁸ N. M. Shaw,²⁹ P. F. Shepard,²⁸ T. Shibayama,³⁷ M. Shimojima,³⁷ M. Shochet,⁵ J. Siegrist,¹⁸ A. Sill,³⁵ P. Sinervo,¹⁴ P. Singh,¹³ K. Sliwa,³⁸ C. Smith,¹⁵ F. D. Snider,¹⁵ J. Spalding,⁷ T. Speer,¹⁰ P. Sphicas,¹⁹ F. Spinella,²⁷ M. Spiropulu,¹¹ L. Spiegel,⁷ L. Stanco,²⁵ J. Steele,⁴⁰ A. Stefanini,²⁷ R. Ströhmer,^{7,*} J. Strologas,¹³ F. Strumia,¹⁰ D. Stuart,⁷ K. Sumorok,¹⁹ J. Suzuki,³⁷ T. Suzuki,³⁷ T. Takahashi,²⁴ T. Takano,²⁴ R. Takashima,¹² K. Takikawa,³⁷ M. Tanaka,³⁷ B. Tannenbaum,²² F. Tartarelli,²⁷ W. Taylor,¹⁴ M. Tecchio,²⁰ P. K. Teng,³³ Y. Teramoto,²⁴ K. Terashi,³⁷ S. Tether,¹⁹ D. Theriot,⁷ T. L. Thomas,²² R. Thurman-Keup,¹ M. Timko,³⁸ P. Tipton,³⁰ A. Titov,³¹ S. Tkaczyk,⁷ D. Toback,⁵ K. Tollefson,¹⁹ A. Tollestrup,⁷ H. Toyoda,²⁴

W. Trischuk,¹⁴ J. F. de Troconiz,¹¹ S. Truitt,²⁰ J. Tseng,¹⁹ N. Turini,²⁷ T. Uchida,³⁷ F. Ukegawa,²⁶ J. Valls,³² S. C. van den Brink,²⁸ S. Vejcik III,²⁰ G. Velev,²⁷ R. Vidal,⁷ R. Vilar,^{7,*} D. Vucinic,¹⁹ R. G. Wagner,¹ R. L. Wagner,⁷ J. Wahl,⁵ N. B. Wallace,²⁷ A. M. Walsh,³² C. Wang,⁶ C. H. Wang,³³ M. J. Wang,³³ A. Warburton,¹⁴ T. Watanabe,³⁷ T. Watts,³² R. Webb,³⁴ C. Wei,⁶ H. Wenzel,¹⁶ W. C. Wester III,⁷ A. B. Wicklund,¹ E. Wicklund,⁷ R. Wilkinson,²⁶ H. H. Williams,²⁶ P. Wilson,⁵ B. L. Winer,²³ D. Winn,²⁰ D. Wolinski,²⁰ J. Wolinski,²¹ S. Worm,²² X. Wu,¹⁰ J. Wyss,²⁷ A. Yagil,⁷ W. Yao,¹⁸ K. Yasuoka,³⁷ G. P. Yeh,⁷ P. Yeh,³³ J. Yoh,⁷ C. Yosef,²¹ T. Yoshida,²⁴ I. Yu,⁷ A. Zanetti,³⁶ F. Zetti,²⁷ and S. Zucchelli²

(CDF Collaboration)

¹Argonne National Laboratory, Argonne, Illinois 60439

²Istituto Nazionale di Fisica Nucleare, University of Bologna, I-40127 Bologna, Italy

³Brandeis University, Waltham, Massachusetts 02254

⁴University of California at Los Angeles, Los Angeles, California 90024

⁵University of Chicago, Chicago, Illinois 60637

⁶Duke University, Durham, North Carolina 27708

⁷Fermi National Accelerator Laboratory, Batavia, Illinois 60510

⁸University of Florida, Gainesville, Florida 32611

⁹Laboratori Nazionali di Frascati, Istituto Nazionale di Fisica Nucleare, I-00044 Frascati, Italy

¹⁰University of Geneva, CH-1211, Geneva 4, Switzerland

¹¹Harvard University, Cambridge, Massachusetts 02138

¹²Hiroshima University, Higashi-Hiroshima 724, Japan

¹³University of Illinois, Urbana, Illinois 61801

¹⁴Institute of Particle Physics, McGill University, Montreal, Canada H3A 2T8
and University of Toronto, Toronto, Canada M5S 1A7

¹⁵The Johns Hopkins University, Baltimore, Maryland 21218

¹⁶Institut für Experimentelle Kernphysik, Universität Karlsruhe, 76128 Karlsruhe, Germany

¹⁷National Laboratory for High Energy Physics (KEK), Tsukuba, Ibaraki 305, Japan

¹⁸Ernest Orlando Lawrence Berkeley National Laboratory, Berkeley, California 94720

¹⁹Massachusetts Institute of Technology, Cambridge, Massachusetts 02139

²⁰University of Michigan, Ann Arbor, Michigan 48109

²¹Michigan State University, East Lansing, Michigan 48824

²²University of New Mexico, Albuquerque, New Mexico 87131

²³The Ohio State University, Columbus, Ohio 43210

²⁴Osaka City University, Osaka 588, Japan

²⁵Università di Padova, Istituto Nazionale di Fisica Nucleare, Sezione di Padova, I-35131 Padova, Italy

²⁶University of Pennsylvania, Philadelphia, Pennsylvania 19104

²⁷Istituto Nazionale di Fisica Nucleare, University and Scuola Normale Superiore of Pisa, I-56100 Pisa, Italy

²⁸University of Pittsburgh, Pittsburgh, Pennsylvania 15260

²⁹Purdue University, West Lafayette, Indiana 47907

³⁰University of Rochester, Rochester, New York 14627

³¹Rockefeller University, New York, New York 10021

³²Rutgers University, Piscataway, New Jersey 08855

³³Academia Sinica, Taipei, Taiwan 11530, Republic of China

³⁴Texas A&M University, College Station, Texas 77843

³⁵Texas Tech University, Lubbock, Texas 79409

³⁶Istituto Nazionale di Fisica Nucleare, University of Trieste, Udine, Italy

³⁷University of Tsukuba, Tsukuba, Ibaraki 315, Japan

³⁸Tufts University, Medford, Massachusetts 02155

³⁹Waseda University, Tokyo 169, Japan

⁴⁰University of Wisconsin, Madison, Wisconsin 53706

⁴¹Yale University, New Haven, Connecticut 06520

(Received 2 September 1998)

We describe a measurement of the charge asymmetry of leptons from W -boson decays in the rapidity range $0 < |y_l| < 2.5$ using $W \rightarrow e\nu, \mu\nu$ events from $110 \pm 7 \text{ pb}^{-1}$ of data collected by the CDF detector during 1992–1995. The asymmetry data constrain the ratio of d and u quark momentum distributions in the proton over the x range of 0.006 to 0.34 at $Q^2 \approx M_W^2$. The asymmetry predictions that use parton distribution functions obtained from previously published CDF data in the central rapidity region ($0.0 < |y_l| < 1.1$) do not agree with the new data in the large rapidity region ($|y_l| > 1.1$). [S0031-9007(98)08026-0]

PACS numbers: 13.85.Qk, 13.38.Be, 14.70.Fm

At Fermilab Tevatron energies, $W^+(W^-)$ bosons are produced in $p\bar{p}$ collisions primarily by the annihilation of u (d) quarks in the proton and \bar{d} (\bar{u}) quarks from the antiproton. Because u quarks carry on average more momentum than d quarks [1–3], the W^+ bosons tend to follow the direction of the incoming proton and the W^- bosons that of the antiproton. The charge asymmetry in the production of W bosons is related to the u and d quark distributions at $Q^2 \approx M_W^2$, and is roughly proportional [4,5] to the ratio of the difference to the sum of the quantities $\frac{d}{u}(x_1)$ and $\frac{d}{u}(x_2)$, where x_1 and x_2 are the fractions of the nucleon's momentum carried by the quarks in the p and \bar{p} , respectively. $\frac{d}{u}(x)$ is the ratio of the d to u quark parton distribution functions for quarks carrying a momentum fraction, x , of the nucleon's momentum.

W asymmetry measurements [6] from 20 pb $^{-1}$ of data collected by the Collider Detector at Fermilab (CDF) in 1992–1993 demonstrated the measurement to be more sensitive than deep inelastic scattering experiments to the $\frac{d}{u}$ ratio within the x range accessible by the W data at the Tevatron. These data contribute to global analyses used to extract parton distribution functions (PDFs) in the nucleon [1–3]. These functions are used in the calculation of all hadronic cross sections. CDF's previous asymmetry data [6] improved the understanding of the u and d quark momentum distributions in the proton in the x range $0.007 < x < 0.24$. The use of these data resulted in a reduction in the uncertainty from PDFs in the W mass measurement [7] from ≈ 75 to ≈ 50 MeV/ c^2 . A further reduction of this error to ≈ 20 MeV/ c^2 is possible [8] using the new data presented here. Recently fixed target Drell-Yan data [9] has also been used to constrain the ($u - d$) sea quark distribution.

In this Letter, we describe the asymmetry results at $\sqrt{s} = 1.8$ TeV using data from the entire 1992–1995 period, using a total integrated luminosity of 110 ± 7 pb $^{-1}$ —a 5-fold increase relative to the 1992–1993 data. The new measurements agree with and supersede the previous results. The asymmetry measurement is extended to larger rapidity [10] ($|y_l| < 2.4$) by the introduction of a new charge determination technique [11] for electrons, and also by using data from the forward muon detector ($1.9 < |y_l| < 2.5$). These electron and muon data at large rapidity provide information about PDFs for a larger x range ($0.006 < x < 0.34$) than previously available. The mean x values of the d and u parton distributions probed by the CDF asymmetry data are shown in Table I.

Since the W rapidity is experimentally undetermined because of the unknown longitudinal momentum of the neutrino from the W decay, we measure the lepton charge asymmetry which is a convolution of the W production charge asymmetry and the $V - A$ asymmetry from the W decay. The two asymmetries tend to cancel at large values ($|y_l| \geq 2$) of rapidity. However, if one assumes W decays proceed via a pure $V - A$ interaction, the lepton asymmetry is still sensitive to the parton distribution

TABLE I. The mean x values of the d and u parton distributions probed by the CDF asymmetry data for the W^+ boson as a function of the lepton rapidity. The $\frac{d}{u}$ ratios from the CTEQ-3M parametrization are shown for these x values. The mean x values for the W^- at positive y_l are the same as those for the W^+ at the same negative y_l .

$\langle y_l \rangle$	$\langle x_u \rangle$	$\langle x_d \rangle$	$\frac{d}{u}(x_u)$	$\frac{d}{u}(x_d)$
-2.20	0.009	0.219	0.911	0.412
-1.54	0.016	0.129	0.864	0.542
-1.10	0.021	0.088	0.837	0.625
-0.49	0.038	0.051	0.765	0.722
0.00	0.044	0.044	0.744	0.744
0.49	0.099	0.021	0.601	0.837
1.10	0.165	0.012	0.483	0.889
1.54	0.225	0.009	0.405	0.911
2.20	0.335	0.006	0.306	0.936

functions. The lepton charge asymmetry is defined as

$$A(y_l) = \frac{d\sigma^+/dy_l - d\sigma^-/dy_l}{d\sigma^+/dy_l + d\sigma^-/dy_l}, \quad (1)$$

where $d\sigma^+(d\sigma^-)$ is the cross section for $W^+(W^-)$ decay leptons as a function of lepton rapidity, with positive rapidity being defined in the proton beam direction. If the detection efficiencies and acceptances for l^+ and l^- are equal, then the uncertainties on these quantities do not affect $A(y_l)$.

The tracking detectors at CDF [12] are the Vertex Time Projection Chambers (VTX), the Central Tracking Chamber (CTC, $|\eta| < 1.8$), the Silicon Vertex Detector (SVX, $|\eta| < 2.3$), the Central Muon Chambers (CMU and CMX, $|\eta| < 1.0$), and the Forward Muon Detector (FMU, $1.9 < |\eta| < 3.5$). The VTX provides r - z tracking information out to a radius of 22 cm for $|\eta| < 3.25$ and is used to measure the z location [10] of the primary interaction vertex. The CTC is an 84 layer drift chamber inside the 1.4 T solenoidal magnet which provides the curvature measurement of electrons and muons from W decays. The CTC has a momentum resolution of $\delta(1/p_T) = 0.00081(\text{GeV}/c)^{-1}$ [7]. The SVX is a 51 cm long, 4 layer precision vertex detector with a track position resolution [11] of ≈ 10 μm . Because $p\bar{p}$ interactions at CDF are spread along the beam line with an RMS of ≈ 30 cm, the geometrical acceptance of the SVX is about 60% for W candidate events. In this analysis, the SVX complements the CTC for electron tracking at high $|\eta|$ ($1.2 < |\eta| < 2.3$). The FMU consists of two steel magnets (toroids) alternately inserted between 3 drift chambers.

W decays to leptons are identified by a charged track pointing either at hits in the muon chambers or a cluster of energy in the electromagnetic (EM) calorimeters accompanied by large missing transverse energy (\cancel{E}_T) [10]. Electron candidates are required to fall within the fiducial regions of either the central ($|y_l| < 1.1$) or the plug ($1.1 < |y_l| < 2.4$) EM calorimeters and to pass

identification cuts based on the EM shower's profile determined with test beam electrons. Muon candidates are required to have a track in the muon tracking system and a minimum ionizing particle signal in the hadronic and EM calorimeters. The transverse energy (E_T) of the lepton and \cancel{E}_T are required to be greater than 25 GeV. To further reduce the background from dijet events where one jet is incorrectly reconstructed as a charged lepton and where a large \cancel{E}_T results from shower fluctuations or uninstrumented regions in the detector, events with a jet [13] with $E_T^{\text{jet}} > 30$ GeV are rejected.

The data are divided into five samples: central electrons ($|y_l| < 1.1$), central muons ($|y_l| < 1.0$), plug electrons within the SVX fiducial region (plug-SVX, $1.1 < |y_l| < 2.4$), plug electrons outside the SVX geometrical acceptance region but with a CTC track (plug CTC, $1.1 < |y_l| < 1.8$), and forward muons ($1.9 < |y_l| < 2.5$). In total 88 047 events are selected. A reliable charge determination and a good energy measurement are essential for this analysis. Central electrons, central muons, and plug electrons outside the SVX are required to have an associated CTC track. A reliable charge determination is ensured by a CTC track curvature (C) significance requirement of $C/\delta C > 2$ (where δC is the error in the curvature measurement). The charge of forward muons is measured well in the FMU toroidal magnets. The energy of plug electrons is measured by the EM calorimeters, and the η and ϕ are measured by the tower segmentation [10]. However, tracking information is needed in order to determine the charge. The geometrical acceptance of the plug calorimeters is only partially covered by the CTC. Therefore, the efficiency for finding a CTC track, and hence determining the charge, drops quickly as a function of rapidity and becomes zero for $|y_l| > 1.8$.

A new charge determination technique [11] is introduced to identify the charge of plug electrons within the SVX geometrical fiducial region. At CDF, positively (negatively) charged particle trajectories are bent in increasing (decreasing) ϕ inside the solenoidal magnetic field. The SVX track stub measures precisely the initial track direction in ϕ . The plug EM (PEM) calorimeter [14] shower centroid measurement combined with the location of the vertex position yields another measurement of ϕ , and the sign of the difference of the two ϕ measurements determines the charge. The shower centroid is measured with a strip position detector placed at shower maximum in the pseudorapidity region between 1.2–1.8. In the pseudorapidity region between 1.8–2.4, where there is no strip detector coverage, the centroid is measured from the calorimeter tower information in η and ϕ . We define the ratio $R = \delta\phi_{\text{measured}}/|\delta\phi_{\text{expected}}|$, where $\delta\phi_{\text{measured}} = \phi_{\text{PEM}} - \phi_{\text{SVX}}$, and $\delta\phi_{\text{expected}}$ is calculated from the calorimeter energy, the radial location of the electron shower, and the magnetic field strength. R peaks at +1 and -1 for positrons and electrons, respectively. The measurement error on R is 0.3, 0.5, and 0.8 for $|y_l|$ bins centered at 1.3, 1.8, and 2.2, respectively.

This technique effectively doubles the number of plug electrons that can be used in the measurement and extends the charge measurement to $|y_l| = 2.4$.

A possible charge or E_T dependence of each trigger is investigated by using data from several independent triggers. No evidence of charge dependence is found in the electron and central muon data samples. The forward muon data taken with the toroid polarities set to focus μ^+ and μ^- , respectively, are averaged to cancel out effects of any charge bias in the trigger from geometrical acceptance and alignment errors. The efficiency of the plug electron triggers does not depend on charge, but is not 100% at E_T of 25 GeV. At $E_T = 25$ GeV the average trigger efficiency for the plug-SVX sample is 78%. A correction is applied to the measured asymmetry in each rapidity bin, using a Monte Carlo calculation and the measured trigger efficiency as a function of E_T and y_l . The correction to $A(y_l)$ is found to be less than 0.005 compared with a typical statistical error of 0.015 in the PEM region.

Sources of charge bias in the event selection are investigated by selecting high E_T leptons from either a sample of Z or W events, which satisfy tight kinematic constraints. No charge-dependent bias in acceptance or efficiencies has been found. The charge misidentification rate for muons is negligible. The electron charge misidentification rate (e.g., due to multiple tracks from conversion of Bremsstrahlung photons) in the central region is determined from the rate of same sign central-central Z electrons. In the plug region, the rates are determined from W electron data using the number of events outside the two peaks in the R distribution. This is checked against the same sign central-plug Z electrons as a function of rapidity. The electron charge misidentification rate ranges from 0.2% in the central data sample to 10% in the largest rapidity bin ($|y_l| = 2.20$) of the plug electron data. The charge misidentification rate in the FMU sample is $< 1\%$. The effect of the charge misidentification acts to dilute the charge asymmetry and is corrected on a bin by bin basis.

All backgrounds have been investigated and found to be small (see Table II). The average $W \rightarrow \tau\nu$ background is $2.0\% \pm 0.2\%$ where the error accounts for the small rapidity dependence. In the plug electron sample, the background from misidentified dijet events is the largest. This background is charge symmetric and dilutes the asymmetry. In the central electron sample, the background from $W \rightarrow \tau\nu \rightarrow e\nu\nu\nu$ is the largest. For the central muon sample the largest background is misidentified $Z \rightarrow \mu^+\mu^-$ where one of the muons is outside the acceptance of the CTC. In the latter two cases, the backgrounds are not charge symmetric and the corrections are made using the asymmetry estimated by Monte Carlo calculations. The background from misidentified Z decays to electrons is negligible because the EM calorimeters have a much larger geometric acceptance than the muon chambers or the CTC. In the forward muon sample the background from Z events is 6.5% and the charge-symmetric background totals 8%, of which half is

TABLE II. Backgrounds (%) in the $W \rightarrow e\nu$ and $W \rightarrow \mu\nu$ charge asymmetry event samples.

Sample	QCD dijets	$Z \rightarrow e^+e^-$ or $\mu^+\mu^-$
Central e	0.7 ± 0.2	<0.2
Central μ	0.6 ± 0.2	4.7 ± 0.7
Plug-SVX e	1.6 ± 0.3	<0.2
Plug-CTC e	2.4 ± 0.6	<0.2
Forward μ	4 ± 2	6.5 ± 0.6

from dijets and half from lower p_T muons which are misreconstructed because of random extra hit background in the forward drift chambers. The $Z \rightarrow \tau^+\tau^-$ contamination is negligible. The background from cosmic rays in the muon sample is $<0.2\%$. The $A(y_l)$ values are corrected for the backgrounds on a bin by bin basis.

By CP invariance the asymmetry at positive y_l is equal in magnitude and opposite in sign to that at negative y_l allowing the two measurements to be combined. Figure 1 shows the fully corrected asymmetry after taking the weighted mean of the various data sets and combining the positive and negative y_l bins. The asymmetry and uncertainties are listed in Table III. Figure 1 shows the predictions of quantum chromodynamics (QCD) calculated to next-to-leading order using the program DYRAD [15] with several parametrizations of parton distribution functions as input. The MRS-R2 [16] and CTEQ-3M [2] PDFs have been extracted with the inclusion of the 1992–1993 asymmetry data in their global fits (the 1992–1993 data constitutes 20% of the sample reported here). As shown in Fig. 1, the predictions using these PDFs are in good agreement with the present data in the central region ($|y_l| < 1.1$), with χ^2 per degree of freedom (d.o.f.) values in the range 0.7–1.3. However, at high rapidity, these predictions are generally higher than the data, with $\chi^2/\text{d.o.f.}$ values in the range 5–10, indicating that the PDF parametrizations should be modified in the range $0.006 < x < 0.34$ (see Table I). A recent reanalysis [17] of NMC muon scattering data [18] on hydro-

gen and deuterium with improved corrections for nuclear binding effects in the deuteron has shown the need for a correction to the $\frac{d}{u}$ ratio of the form: $\delta(\frac{d}{u}) = 0.1(x + x^2)$. The prediction using the corrected MRS-R2 PDF is shown in Fig. 1 and shows reasonable agreement with the measured asymmetry at high $|y_l|$. Recent global parton distribution fits [19] (e.g., MRST) that have incorporated the data presented in this paper also lead to agreement at high $|y_l|$. The theoretical uncertainties arising from the effect of the finite charm quark mass [20] are much smaller than the measurement errors.

The W decay lepton charge asymmetry is mostly sensitive to the $\frac{d}{u}$ ratio. However, at large rapidity it is also affected by the W production p_T spectrum. The DYRAD calculation does not reproduce the production p_T spectrum of W events at low p_T . Therefore, it is necessary to check how well the DYRAD calculation compares to one more suitable for the low W p_T region. The DYRAD prediction is compared to a calculation including soft gluon resummation at all orders in perturbation theory implemented in the program REBOS [21]. Both programs yield identical results for the W rapidity distribution, but different results for the W p_T distribution. At Tevatron energies soft gluon radiation is mainly responsible for the p_T of W bosons in the range of $p_T < 30 \text{ GeV}/c$, and REBOS can reproduce the p_T spectrum of W bosons [22]. Figure 1 shows the comparison between the asymmetry predictions of the DYRAD and REBOS programs using CTEQ-3M [2] PDFs. The two calculations agree very well in the central region ($|y_l| < 1.1$), which is the region used in the W mass determination [7]. The difference between the two calculations is mainly at $|y_l| > 1.7$, as illustrated in Fig. 1.

In summary, the asymmetry data demonstrate the value of collider data in the measurement of parton distribution functions and place the strongest constraint on the $\frac{d}{u}$ ratio of quark momentum distributions in the proton over the range x of 0.006 to 0.34 at $Q^2 \approx M_W^2$. The data indicate the need for modifications in the $\frac{d}{u}$ ratio in the PDFs constrained by the previous CDF asymmetry data.

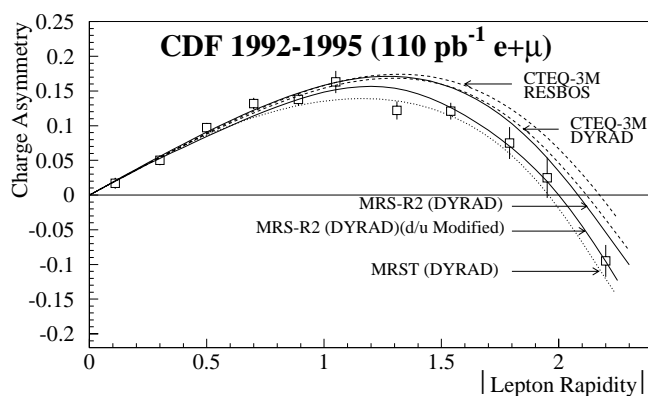


FIG. 1. The fully corrected charge asymmetry. Data from all the detectors for positive and negative y_l are combined. The statistical and systematic errors are added in quadrature.

TABLE III. The charge asymmetries (after all corrections) and statistical and systematic uncertainties in the combined e and μ channels.

$\langle y_l \rangle$	$A(y_l)$	σ_{sys}	$\sigma_{\text{stat+sys}}$
0.11	0.017	± 0.000	± 0.008
0.30	0.050	± 0.000	± 0.007
0.50	0.097	± 0.000	± 0.007
0.70	0.132	± 0.001	± 0.008
0.89	0.138	± 0.001	± 0.009
1.05	0.163	± 0.002	± 0.016
1.31	0.122	± 0.002	± 0.013
1.54	0.121	± 0.003	± 0.012
1.79	0.075	± 0.005	± 0.023
1.95	0.025	± 0.010	± 0.029
2.20	-0.095	± 0.015	± 0.023

We thank the Fermilab staff and the technical staffs of the participating institutions for their vital contributions. This work was supported by the U.S. Department of Energy and National Science Foundation, the Italian Istituto Nazionale di Fisica Nucleare, the Ministry of Education, Science and Culture of Japan, the Natural Sciences and Engineering Research Council of Canada, the National Science Council of the Republic of China, the A. P. Sloan Foundation, and the Swiss National Science Foundation.

*Visitor.

- [1] A. D. Martin *et al.*, Phys. Rev. D **50**, 6734 (1994).
 [2] H. L. Lai *et al.*, Phys. Rev. D **51**, 4763 (1995).
 [3] M. Glück *et al.*, Z. Phys. C **67**, 433 (1995).
 [4] E. L. Berger *et al.*, Phys. Rev. D **40**, 83 (1989); **40**, 3789(E) (1989).
 [5] A. D. Martin *et al.*, Mod. Phys. Lett. A **4**, 1135 (1989).
 [6] F. Abe *et al.*, Phys. Rev. Lett. **74**, 850 (1995).
 [7] F. Abe *et al.*, Phys. Rev. Lett. **75**, 11 (1995).
 [8] M. Lancaster, in *Proceedings of Les Rencontres de Physique de la Vallée d'Aoste, La Thuile, 1997*, edited by M. Greco (INFN, Laboratori Nazionali di Frascati, Frascati, 1998); B. Abbott *et al.*, Phys. Rev. Lett. **80**, 3008 (1997).
 [9] E. A. Hawker *et al.*, Phys. Rev. Lett. **80**, 3715 (1998); A. Baldit *et al.*, Phys. Lett. B **332**, 244 (1994).
 [10] In the CDF coordinate system, θ is the polar angle with respect to the proton beam direction and ϕ is the azimuthal angle. The pseudorapidity η is defined as $-\ln \tan(\theta/2)$ and the lepton rapidity (y_l) as $\ln \frac{E+E_z}{E-E_z}$. Transverse energy is defined as $E_T = E \sin \theta$, where E is the lepton energy. The missing transverse energy, \cancel{E}_T , is defined as the magnitude of the vector sum of E_T in all calorimeter cells with $|\eta| < 3.6$, and including any muon p_T .
 [11] Q. Fan and A. Bodek, in *Proceedings of VIth International Conference on Calorimetry in High Energy Physics, Frascati, Italy 1996* (INFN, Laboratori Nazionali di Frascati, Frascati, 1997); FERMILAB-CONF-96/411-E.
 [12] F. Abe *et al.*, Nucl. Instrum. Methods Phys. Res., Sect. A **271**, 387 (1988), and references therein.
 [13] The jet energy is clustered using a cone algorithm with radius $\Delta R = \sqrt{\Delta\eta^2 + \Delta\phi^2} = 0.7$.
 [14] Y. Fukui *et al.*, Nucl. Instrum. Methods Phys. Res., Sect. A **267**, 280 (1988).
 [15] W. Giele *et al.*, Nucl. Phys. **B403**, 633 (1993).
 [16] A. D. Martin *et al.*, Phys. Lett. B **387**, 419 (1996).
 [17] U. K. Yang, A. Bodek, and Q. Fan, in *Proceedings of the Moriond Conference, QCD and High Energy Hadron Interactions, Les Arcs, France, 1998*, edited by J. Tran Thanh Van (Editions Frontieres, Gif sur Yvette, 1998).
 [18] M. Arneodo *et al.*, Nucl. Phys. **B487**, 3 (1997).
 [19] A. D. Martin *et al.*, Eur. Phys. J. C **4**, 463 (1998).
 [20] S. Kretzer *et al.*, Phys. Lett. B **348**, 628 (1995).
 [21] C. Balazs *et al.*, Phys. Lett. B **355**, 548 (1995).
 [22] B. Abbott *et al.*, Phys. Rev. Lett. **80**, 5498 (1998).